SF2A 2007
J. Bouvier, A. Chalabaev, C. Charbonnel (eds)

JOVIAN S-BURSTS AS MARKERS OF ELECTRON ACCELERATION BY ALFVEN WAVES.

F. Mottez[1], S. Hess[1,2] and P. Zarka[2]

Abstract. Jupiters radio emissions are dominated in intensity by decametric radio emissions due to the Io-Jupiter interaction. Previous analyses suggest that these emissions are cyclotron-maser emissions in the flux tubes connecting Io or Io's wake to Jupiter. Electrons responsible for the emission are thought to be accelerated from Io to Jupiter. We present simulations of this hot electron population under the assumption of acceleration by Alfvèn waves in the Io flux tube (IFT). Outside of limited acceleration regions where parallel electric field associated with Alfvèn waves exists, the electrons are supposed to have an adiabatic motion along the magnetic field lines. Near Jupiter, a loss cone appears in the magnetically mirrored electron population, which is able to amplify extraordinary (X) mode radio waves. The X-mode growth rate is computed, which allows us to build theoretical dynamic spectra of the resulting Jovian radio emissions, whose characteristics match those observed for Jovian S-bursts.

1 Introduction

Io, the closest large satellite of Jupiter, is subject to an intense volcanic activity that almost continuously recycles its atmosphere. Io orbits in the inner magnetosphere of Jupiter where the plasma is in co-rotation with the giant planet. The magnetospheric plasma sweeps the satellite's atmosphere, resulting in a torus of denser cold ($T \sim 5$ eV) and hot (200 eV) plasmas that encompasses the volume defined by the satellite's orbit. Moreover, the magnetic flux tube conecting Io and Jupiter is an active feature, associated to intense radio emissions in the decametric wavelengths range (Queinnec & Zarka 1998, Hess et al. 2007) and bright UV spots at the Io flux tube (IFT) footprint (Prangé 1996). An example of dynamic spectrum of millisecond bursts is shown in Fig. 1. Many bursts can be seen, with a strongly negative frequency drift rate. These observational features suggest the presence of accelerated particles along the Io-Jupiter flux tube. The electric field generated by Io's motion in the corotating plasma induces electric currents and/or Alfvén waves (Goldreich & Lynden-Bell 1969, Neubauer 1980, Saur 2004, Ergun et al. 2006) which may accelerate electrons in the plasma torus and in the Io flux tube (IFT).

In this paper, we investigate the electron acceleration by Alfvén waves propagating along the IFT and its consequences on the DAM radio emissions: Deduced from a theoretical model (Lysak & Song 2003), the electric field associated to the kinetic Alfvén waves is set in the flux tube. The motion of the electrons is computed. The electron distribution functions are built at various altitudes and times after the arrival of the Alfvén waves. The distribution functions are analysed through the linear theory of the maser-cyclotron, the growth rate is computed as a function of time and altitude. The frequency of emission is the local electron gyrofrequency that directly depends on the altitude. Therefore, we can plot the growth rate of the maser-cyclotron instability in the time-frequency plane, and compare this figure with the dynamic spectrum of the decametric millisecond bursts.

2 Filling the flux tube

The particles are moved in a monodimensional domain along a magnetic field line connecting Io and Jupiter. This domain is near Jupiter and do not reach Io, it is 6.5 jovian radii long, and has 4096 computational cells.

[1] Luth, Observatoire de Paris
[2] Lesia, Observatoire de Paris

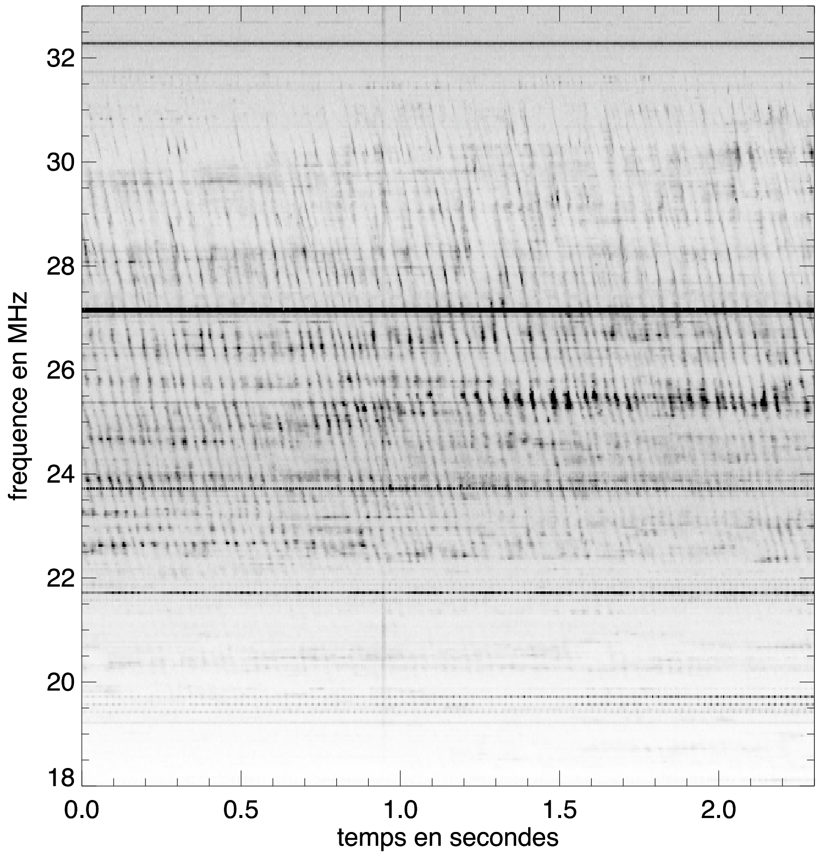

Fig. 1. Dynamic spectrum recorded at the Nançay decameter array. The drifting structures are jovian S-bursts. They show a negative drift rate of about -25 MHz/s, corresponding to the anti-planetward adiabatic motion of the emitting electrons. The bursts are more or less repeated about once every 30 milliseconds. In many other events, the drift and the occurence rate are lower.

The boundary conditions consists of the densities and temperatures for each species, at Io's side boundary and the Jovian ionospheric side. On Jupiter's side, there are cold ionospheric electrons, and protons (0.3 eV). On Io's side, there is a minority of "high energy" 200 eV electrons, a denser population of 5 eV electrons, and warm protons, oxygen II and sulfur II.

The particles are moved along the magnetic field line. The first adiabatic invariant μ is conserved. In the direction along the magnetic field lines, they are subject to the gravitational and electric potentials ϕ_G,ϕ_E. Their equations of motion are

$$\mu = v_\perp^2/B = const. \tag{2.1}$$

$$\frac{dv_\parallel}{dt} = -\nabla(\frac{q}{m}\phi_E + \frac{\mu}{m}B + \phi_G). \tag{2.2}$$

Initially, the box is filled and ϕ_E is computed in a way that fits the boundary conditions and the plasma quasi-neutrality.

3 The Alfvén waves

When a quasi-neutral stationary plasma is settled, an Alfvén wave in injected from the Io boundary. The wave group velocity

$$v_a = (c^2 + \frac{\mu_0\rho}{B^2})^{-1/2} \tag{3.1}$$

and the phase velocity v_ϕ

$$v_\phi = v_a \sqrt{\frac{1 + k_\perp^2 \rho_s^2}{1 + k_\perp^2 \lambda_e^2}} \tag{3.2}$$

depend on the parameters of the plasma filling the IFT (section 2). The perpendicular wavelength $\lambda_\perp$ is proportionnal to the flux tube section (i.e. to $B^{1/2}$) with a value of $\sim 10\ km$ at the jovian surface in our simulation. The parallel electric field generated by a kinetic Alfvén wave has been computed by Lysak and Song (2003). The time and altitude dependency of $\delta E_\parallel$ is displayed on the upper panel of Fig. 3. We can see the propagation toward Jupiter, and after 1.5 second, the reflected Alfvén wave propagating backward.

4 Electron acceleration and distribution functions

The motion of the high energy electrons is then computed according to Eq. (2.1) and (2.2), where the electric potential includes the static electric field contribution and the Alfvén parallel electric field given by the model of Lysak and Song (2003). The electron distribution functions are then computed at various times and altitudes. Fig. 2 shows the electron distribution function at time 3.9 seconds and three different altitudes. We can see a loss cone due to the electron precipitated in the jovian ionosphere, a slight enhancement of energetic electrons, and perturbations of the loss cone due to the particles accelerated by the wave.

5 Maser-cyclotron growth rate

The maser cyclotron growth rate can be deduced, through the linear theory, from the electron distribution function (Wu and Lee 1979, Wu 1985, Galopeau et al. 2004). The resonnance condition is given by

$$\omega = \omega_c/\Gamma - k_\parallel v_\parallel \tag{5.1}$$

where ω is the wave frequency, ω_c the electron cyclotron frequency and Γ the relativistic Lorentz factor. In the weakly relativistic approximation the wave-particle resonance condition is represented by a circle in the $(v_\parallel, v_\perp)$ plane of center v_0 and radius R given by

$$\mathbf{v}_0 = c\frac{\mathbf{k}.\mathbf{b}}{k} \simeq \frac{k_\parallel c^2}{\omega_c}\mathbf{u}_\parallel \tag{5.2}$$

$$R = \sqrt{v_0^2 - 2(\frac{\omega}{\omega_c} - 1)}, \tag{5.3}$$

where $\mathbf{b}$ and $\mathbf{u}_\parallel$ are the unit vectors of the magnetif field and of the parallel velocity.

The solution of the equation of dispersion for non-relativistic particles and for $|\omega| > |\gamma|$ is:

$$\gamma = \frac{\omega_p^2 c^2}{8\omega_c}\int_0^{2\pi} v_\perp^2(\theta)\nabla_{v_\perp} f(\mathbf{v}_0, \mathbf{R}(\theta))d\theta \text{ with } \omega > \omega_c \tag{5.4}$$

The maser instability occurs when $\gamma > 0$, and this requires a positive gradient $\nabla_{v_\perp} f(\mathbf{v}_0, \mathbf{R}(\theta))$ along a section of the resonance circle with a dominant contribution to the integral in equation (5.4). This is the case for "loss-cone" and "shell" distributions. In our simulation we compute the growth rates from the particle distributions along the field line for several resonance circle centers v_0 and radii R (which correspond to several frequencies ω and parallel wave vectors $k_\parallel$). Each of these circles corresponds to an extraordinary mode, many of them are amplified. We retain the mode with the largest growth rate.

In this presentation, we compute the loss cone instability and neglect the shell. We make that choice because, as will be shown in the following section, the loss cone instability is highly sensitive to small variations of the distribution function, and therefore, is time and altitude dependent, as the Jovian millisecond bursts. Therefore, the integral (5.4) is computed along (many) circles that are tangent to the loss cone.

6 Pseudo dynamic spectrum

We obtain a series of dominant growth rates for various times and altitudes. As the emission frequency is very close to the electron gyrofrequency, as this frequency can be deduced from the altitude, we can display the dominant growth rates of the loss cone instability in the same format as a dynamic spectrum. This is shown in Fig 3, in the middle and lower panels. We can see that the growth rate is moderately high during the passage of the Alfvén wave, but, a few seconds alter, it becomes stronger during short laps of time (a few milliseconds) at every altitude. As the maser radiations are more intense when the growth rate is larger (we neglect the effects of nonlinear saturation), we can consider this plot as a kind of model of a dynamical spectrum of the radio emissions. Therefore, it is interesting to compare this plot to a typical dynamical spectrum of millisecond bursts, such as the spectrum shown on Fig 1. We can see that our model allows to reproduce

- the discrete structure of the bursts;
- the frequency drift according to time (mostly with with a negative slope as in 98.5% of real millisecond bursts), that is compatible with the hypothesis of the electron adiabatic motion (conservation of μ all along their trajectory);
- the quasi-periodic occurence of the bursts. This occurence in our model is correlated to the period of the input Alfvén wave. The occurence rate measured on real data is compatible with Alfén waves resonnances frequencies in the vicinity of Jupiter (Su et al 2006).

This similarity between observational data and our plot may support the idea that the millisecond bursts are caused by electrons accelerated by Alfvén waves propagatig along the Io-Jupiter flux tube. In that case, the occurence rate of the millisecond bursts would be a signature of the wave frequency.

References

Ergun, R. E. and Su, Y.-J. and Andersson, L. and Bagenal, F. and Delemere, P. A. and Lysak, R. L. and Strangeway, R. J.. 2006, J. Geophys. Res., 111, 6212

Galopeau, P. H. M. and Boudjada, M. Y. and Rucker, H. O.. 2004, J. Geophys. Res., 109, 12217-+

Goldreich, P. and Lynden-Bell, D.. 1969, Astrophys. J., 156, 59-78

Hess, S., Zarka, P. and Mottez, F., 2007, Planetary and Space Science, 55, 89-99

Lysak, R. L. and Song, Y., 2003, J. Geophys. Res., 108, 1-6

Neubauer, F. M., 1980, J. Geophys. Res., 85, 1171-1178

Prangé, R., Rego, D.,Southwood, D., and Zarka, P.,1996, Nature, 379, 323-325

Queinnec, J. and Zarka, P.. 1998, J. Geophys. Res., 103, 26649-26666

Saur, J., 2004 J. Geophys. Res., 109, 1210

Su, Y.-J. and Jones, S. T. and Ergun, R. E. and Bagenal, F. and Parker, S. E. and Delamere, P. A. and Lysak, R. L., 2006 J. Geophys. Res., 111, 6211-+

Wu, C. S., 1985 Space Science Reviews, 41, 215-298

Wu, C. S. and Lee, L. C., 1979 Astrophys. J., 230, 621-626

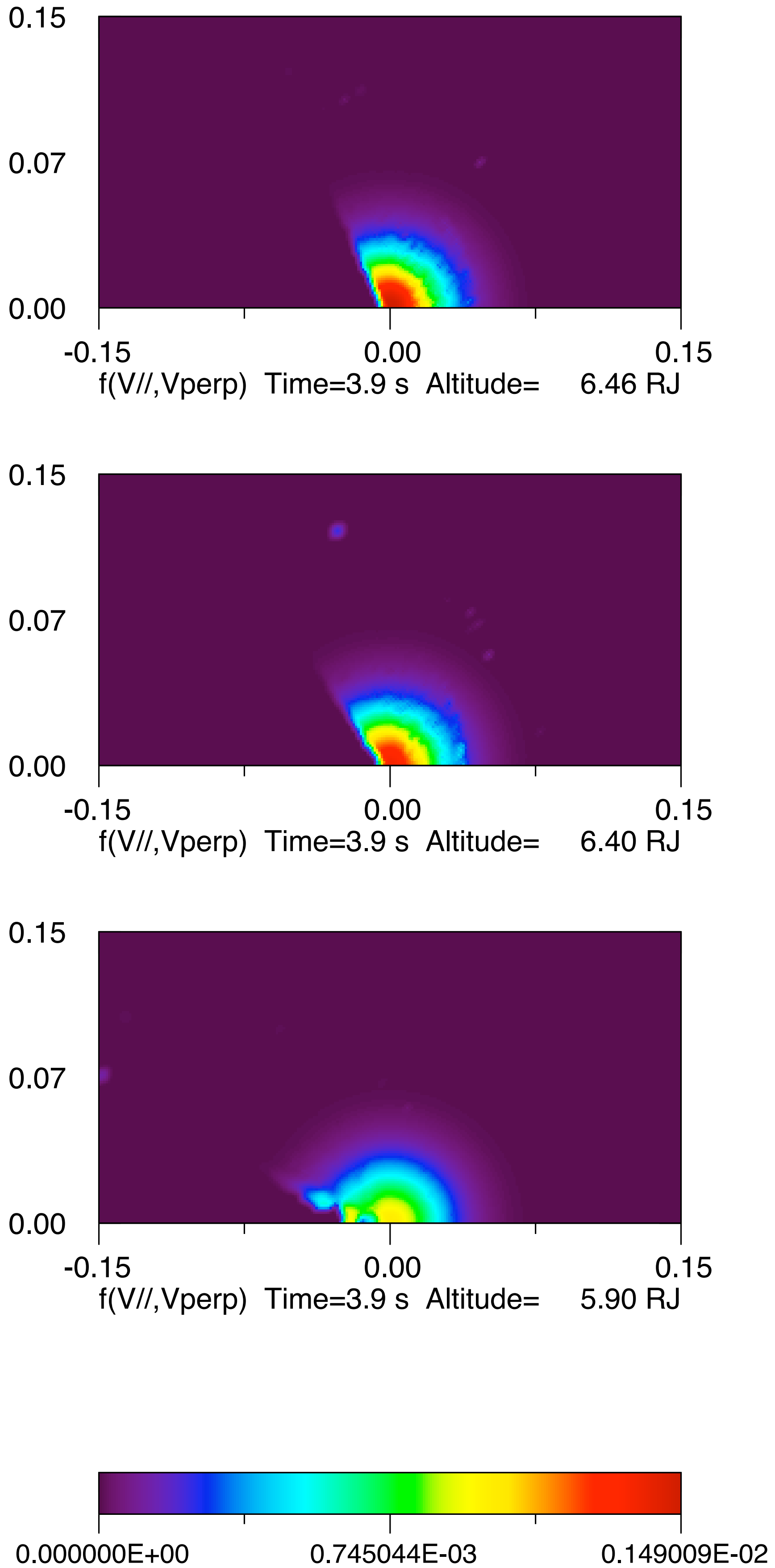

Fig. 2. The electron distribution function $f(v_{\parallel}, v_{\perp})$ at time 3.9 second, and three different altitudes. The altitude is counted from the Io side border of the box, and reaches 6.5 R_J at the jovian ionosphere.

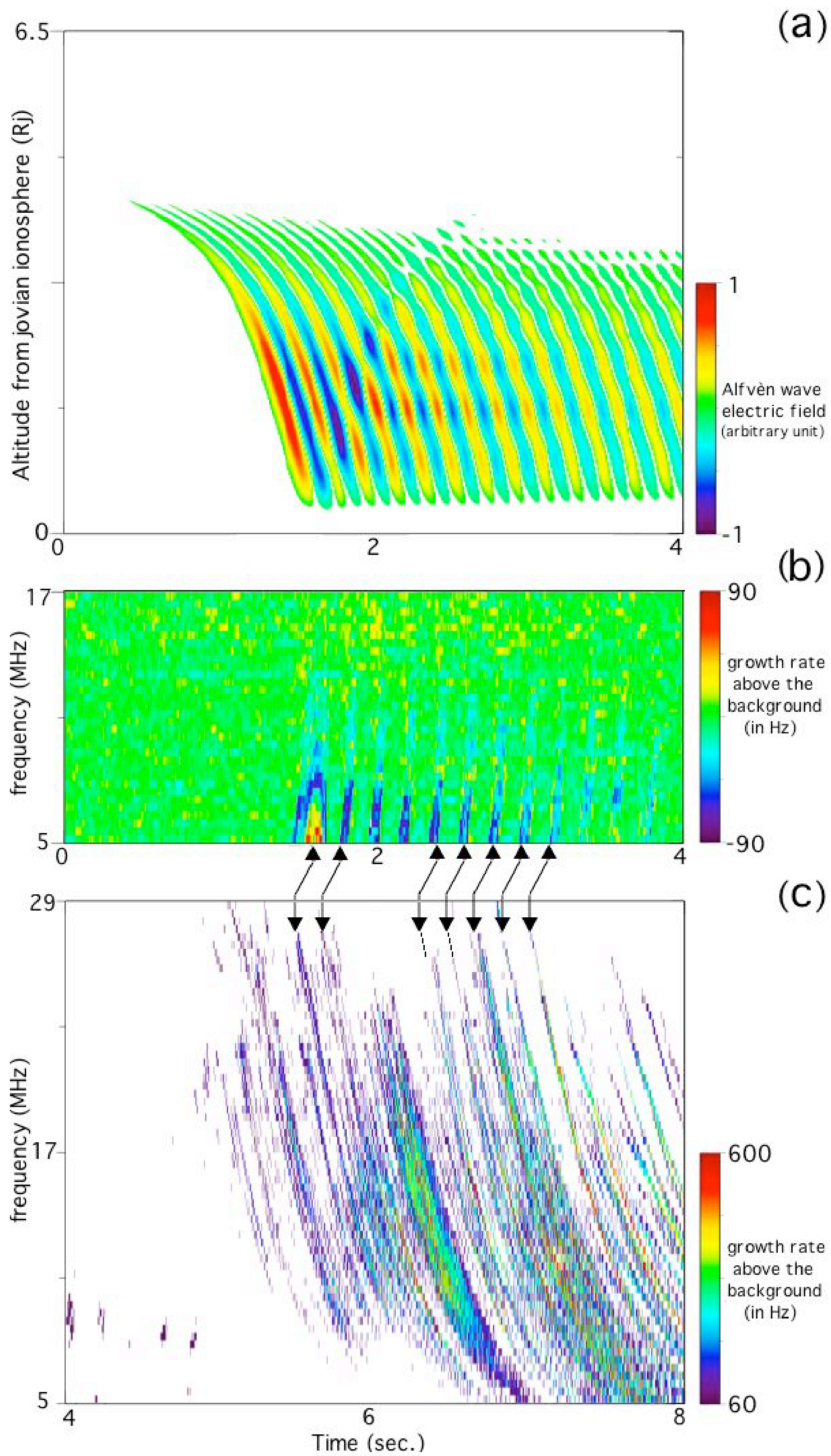

Fig. 3. Various data as functions of time and altitude/frequency. The altitude is counted from the Io side border of the box, and reaches 6.5 R_J at the jovian ionosphere. Upper panel : the parallel Alfvén wave electric field from the model of Lysak and Song (2003), as a function of time and altitude. Middle panel : growth rate of the loss cone instability during the passage of the Alfvén wave. Lower panel : growth rate of the loss cone instability after the passage of the Alfvén wave. (The color scale is different, because the signal is stronger than in the middle panel)